Supporting Information

Facile and gram-scale synthesis of single-crystal hydrogen-bonded organic frameworks as iodine adsorbents for synthesis of β-iodoethers

Zhiye Zheng,[a†] Qiuyuan Lin,[a†] Shunfeng Peng,[a] Yuxuan Zhang,[a] Shuting Xu,[a] Hui Zhang,[b] Hongyu Wang[a]*

[a] Department of Chemistry, College of Science, and Center for Supramolecular Chemistry & Catalysis, Shanghai University, 99 Shangda Road, Shanghai, 200444, P. R. China. E-mail: wanghy@shu.edu.cn

[b] Laboratory for Microstructures, Instrumental Analysis and Research Center, Shanghai University, Shanghai 200444, P. R. China

[†] These authors contributed equally to this work.

Table of contents

Materials and instruments

Unless otherwise stated, all reagents and solvents were obtained from commercial sources and used without further purification. 4-[tris(4-formylphenyl)methyl]benzaldehyde (TFPM) and 1-Butyl-3-methylimidazolium hexafluorophosphate ([BMIm][PF_6]) were purchased from Bide Pharmatech Ltd. (Shanghai, China). *p*-Phenylenediamine (PDA) and 4,4′-diaminobiphenyl (DABP) were purchased from Adamas-Beta. (Shanghai, China). Aqueous solutions of iodine were prepared using deionized water.

The data of diffraction grade single crystals for **H1** were collected on a Bruker D8 Venture diffractometer using a μ-focus Cu Kα radiation source (λ = 1.54178 Å) with collimating mirror monochromators. Nuclear magnetic resonance (NMR) spectra were recorded on a JEOL 400 MHz spectrometer using tetramethylsilane as the internal standard. ^{1}H NMR chemical shifts are reported in δ units, parts per million (ppm), relative to the chemical shift of the residual solvent. Scanning electron microscopy (SEM) images of the HOF samples were performed using a Phenom Pharos Desktop SEM from Thermo Fisher Scientific. Fourier transform infrared (FT-IR) spectra were measured in transmission mode using a Nicolet iS50 spectrometer and KBr pellets at room temperature. Powder X-ray diffraction patterns were recorded on a Rigaku D/Max2500V/PC X-ray powder diffractometer with Cu-Kα radiation (λ = 0.15418 nm). Thermogravimetric analyses (TGA) were carried out on a DSCQ1000 gravimetric thermal analyzer. The surface area and pore size distribution analyses of the polymers were determined using a Quantachrome Autosorb-IQ2 gas adsorption and pore size analyzer, using N_2 adsorption and desorption at 77 K. Samples were degassed at 100 ˚C under vacuum for 24 h prior to each N_2 adsorption and desorption analysis. UV-vis/NIR spectra were recorded on a Perkin-Elmer Lambda 750 spectrometer. Electron paramagnetic resonance (EPR) spectroscopy was carried out on a Bruker EMX Plus spectrometer. Raman spectra were recorded on a Renishaw InVia Raman microscope.

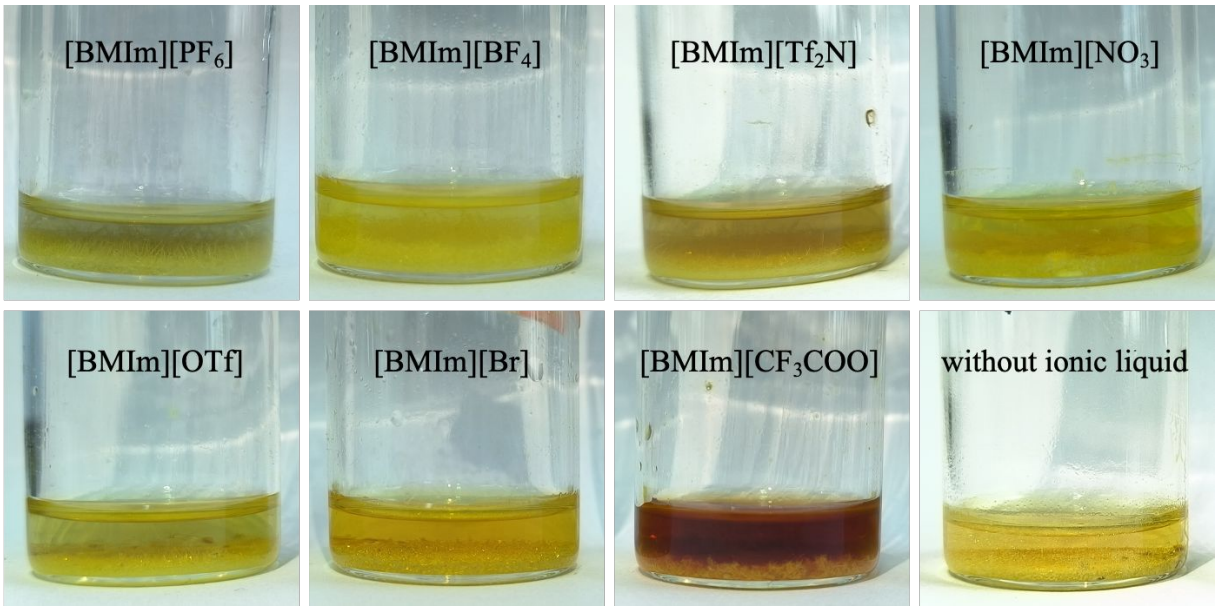

Figure S1. Photographs of the reaction mixture catalyzed by various ionic liquids. Reaction conditions: 1.0 equiv. of TFPM (0.025 mmol), 4.0 equiv. of PDA, IL 0.5 mL, acetonitrile 2 mL, under ambient pressure, 35 °C, 24 h.

Table S1. Synthesis of H1 with various ionic liquid catalysts. [a]

Ionic liquids	Crystal shape	Yield (%)
[BMIm][PF_6]	Long needle	83
[BMIm][BF_4]	Long needle	71.7
[BMIm][Tf_2N]	Long needle	62.6
[BMIm][NO_3]	Short needle	62.6
[BMIm][OTf]	Short needle	30.3
[BMIm][Br]	Small crystal	61.1
[BMIm][CF_3COO]	Short needle	78.3
- [b]	Small crystal	35.4

[a] Reaction conditions: 1.0 equiv. of TFPM (0.025 mmol), 4.0 equiv. of PDA, IL 0.5 mL, acetonitrile 2 mL, under ambient pressure, 35 °C, 24 h. [b] Absence of ionic liquid catalyst.

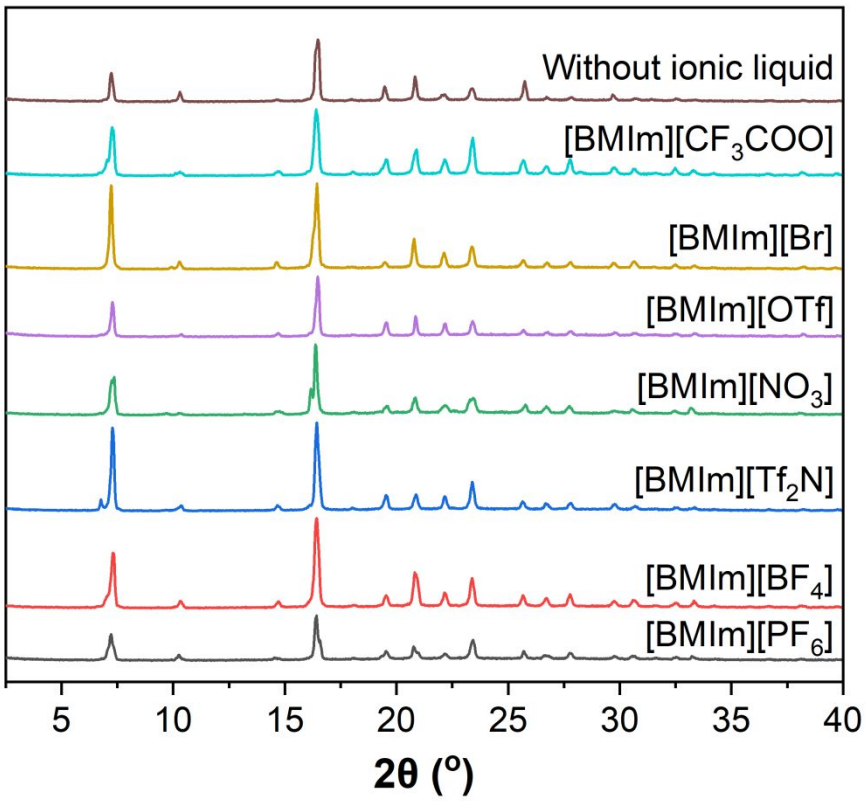

Figure S2. PXRD patterns of **H1** catalyzed by various ionic liquids. Reaction conditions: 1.0 equiv. of TFPM (0.025 mmol), 4.0 equiv. of PDA, IL 0.5 mL, acetonitrile 2 mL, under ambient pressure, 35 °C, 24 h.

Table S2. The effect of solvent on the condensation reaction. [a]

Solvents	Solubility		Protocol	Product
	TFPM	PDA		
Acetonitrile	poor	good	PDA powder was added into the suspension of TFPM in acetonitrile in presence of [BMIm][PF_6]	Long yellow crystal
THF	good	good	PDA powder was added into the solution of TFPM in THF in presence of [BMIm][PF_6]	No solid product
DMF	good	good	PDA powder was added into the solution of TFPM in DMF in presence of [BMIm][PF_6]	No solid product
DMSO	good	good	PDA powder was added into the solution of TFPM in DMSO in presence of [BMIm][PF_6]	No solid product
DMSO/acetonitrile (1 : 1, v : v)	poor	good	PDA powder was added into the suspension of TFPM in DMSO/acetonitrile in presence of [BMIm][PF_6]	No solid product
1,4-dioxane	poor	good	PDA powder was added into the suspension of TFPM in 1,4-dioxane in presence of [BMIm][PF_6]	Amorphous solid
- [b]	poor	poor	PDA powder was added into the suspension of TFPM in [BMIm][PF_6]	No solid product

[a] Reaction conditions: 1.0 equiv. of TFPM (0.025 mmol), 4.0 equiv. of PDA, [BMIm][PF_6] 0.5 mL, solvent 2 mL, under ambient pressure, 35 °C, 24 h. [b] Absence of ionic liquid catalyst.

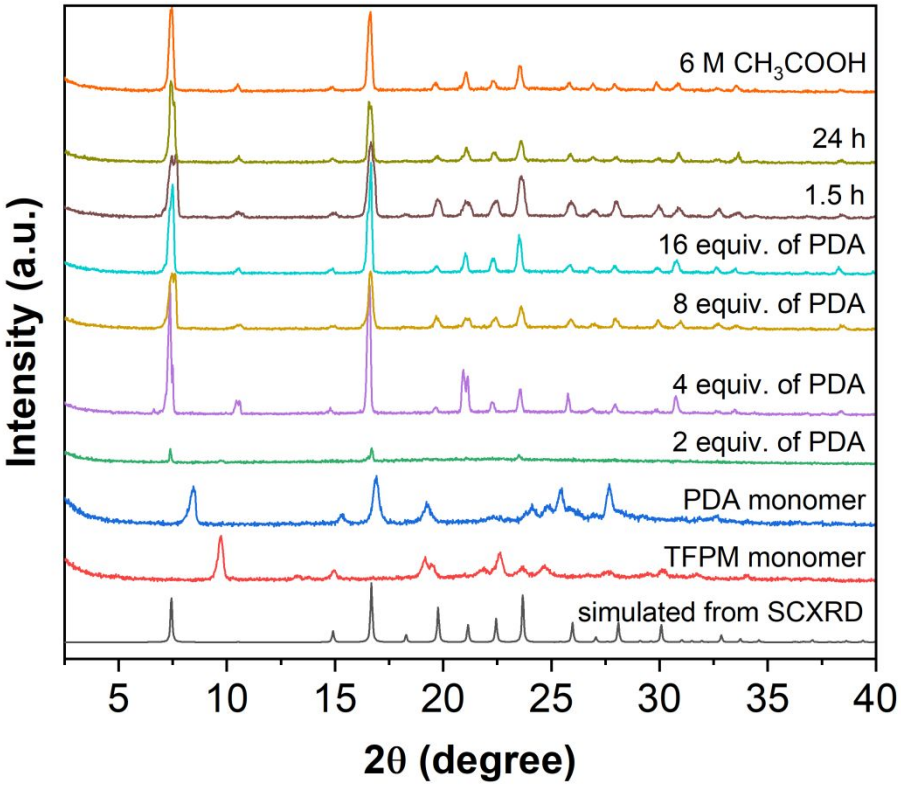

Figure S3. PXRD patterns of **H1** prepared with different feeding ratios and reaction time.

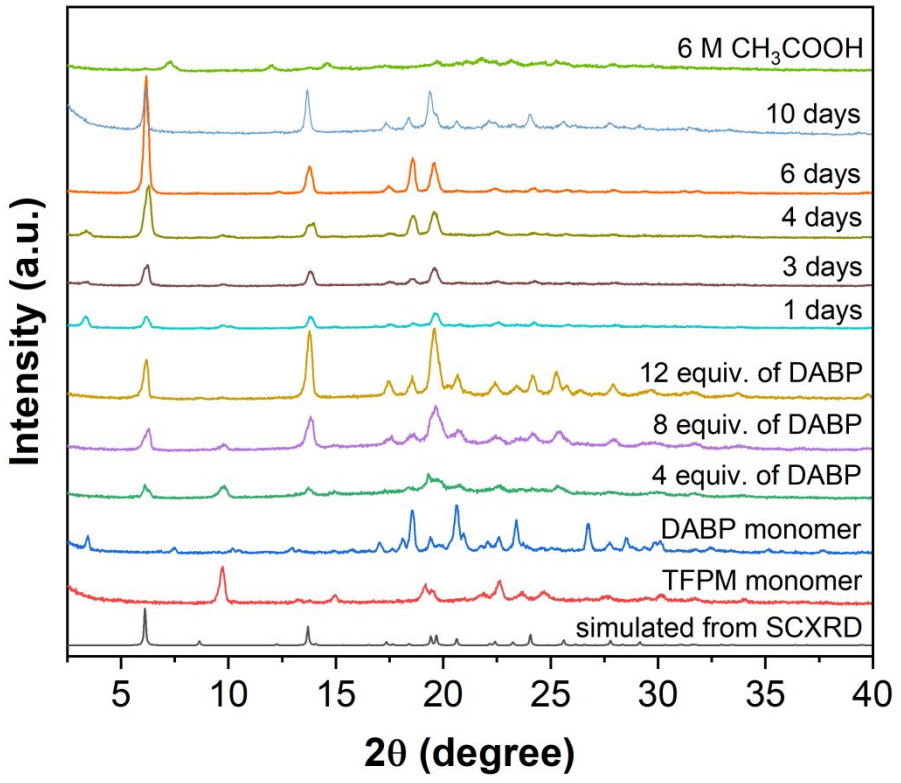

Figure S4. PXRD patterns of **H2** prepared under different reaction conditions.

X-ray experimental for H1 and H2

Diffraction grade single crystals of **H1** and **H2** were obtained by the facile synthesis directly. A suitable crystal was isolated, and the data were collected on a Bruker D8 Venture diffractometer using a μ-focus Cu Kα radiation source (λ = 1.54178 Å) with collimating mirror monochromators. Data were collected using ω-scans. The structures were solved by direct methods using SHELXT and refined by full-matrix least-squares on F^2 with anisotropic displacement parameters for the non-H atoms using SHELXL-2018/3. Structure analysis was aided by use of the programs PLATON and OLEX2.

Table S3. Crystal data and structure refinement for **H1**.

Empirical formula	$C_{53}H_{44}N_8$
Formula weight	792.96 g/mol
Temperature/K	150(2)
Crystal system	Tetragonal
Space group	I 41/a
a/Å	23.7454(13)
b/Å	23.7454(13)
c/Å	7.1607(7)
α/°	90
β/°	90
γ/°	90
Volume/Å^3	4037.5(6)
Z	4
ρ_{calc} g/cm^3	1.305
μ/mm^{-1}	0.612
F(000)	1672
Crystal size/mm^3	0.015 × 0.017 × 0.020
Radiation	Cu Kα (λ = 1.54178 Å)
2Θ range for data collection/°	3.72 to 66.67
Index ranges	-27 ≤ h ≤ 28, -28 ≤ k ≤ 28, -8 ≤ l ≤ 8
Reflections collected	23082
Independent reflections	1793 [R_{int} = 0.1191]
Data/restraints/parameters	1793/0/139
Goodness-of-fit on F^2	1.112
Final R indexes [I>=2σ (I)]	R_1 = 0.0602, wR_2 = 0.1955
Final R indexes [all data]	R_1 = 0.0812, wR_2 = 0.2103
Largest diff. peak/hole / e Å^{-3}	0.394/-0.174
CCDC number	2391554

Table S4. Crystal data and structure refinement for **H2**.

Empirical formula	$C_{77}H_{60}N_8$
Formula weight	1097.33 g/mol
Temperature/K	213.00
Crystal system	Tetragonal
Space group	I 41/a
a/Å	28.8802(6)
b/Å	28.8802(6)
c/Å	7.2054(2)
α/°	90
β/°	90
γ/°	90
Volume/Å^3	6009.8(3)
Z	4
ρ_{calc} g/cm^3	1.213
μ/mm^{-1}	0.354
F(000)	2312
Crystal size/mm^3	0.07 × 0.07 × 0.05
Radiation	Cu Kα (λ = 1.54178 Å)
2Θ range for data collection/°	3.766 to 54.869
Index ranges	-35 ≤ h ≤ 27, -34 ≤ k ≤ 30, -5 ≤ l ≤ 8
Reflections collected	20575
Independent reflections	2840 [R_{int} = 0.0555]
Data/restraints/parameters	2840/0/193
Goodness-of-fit on F^2	1.083
Final R indexes [I>=2σ (I)]	R_1 = 0.0723, wR_2 = 0.2399
Final R indexes [all data]	R_1 = 0.0907, wR_2 = 0.2536
Largest diff. peak/hole / e Å^{-3}	0.323/-0.390
CCDC number	2391555

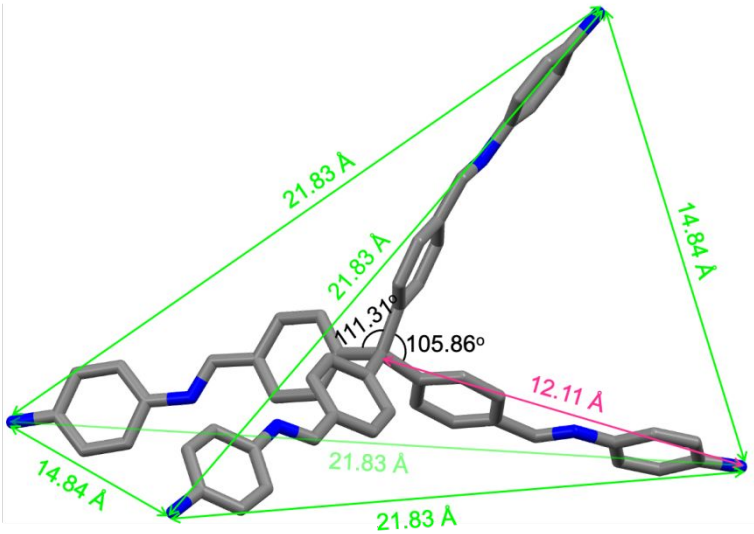

Figure S5. The single crystal molecular structure of **H1** displaying a quasi-tetrahedral conformation (C: gray, N: blue). Hydrogen atoms are omitted for clarity. The green lines show the distances between the terminal nitrogen atoms. The pink line shows the distance between the central methane carbon atom and the terminal nitrogen atoms.

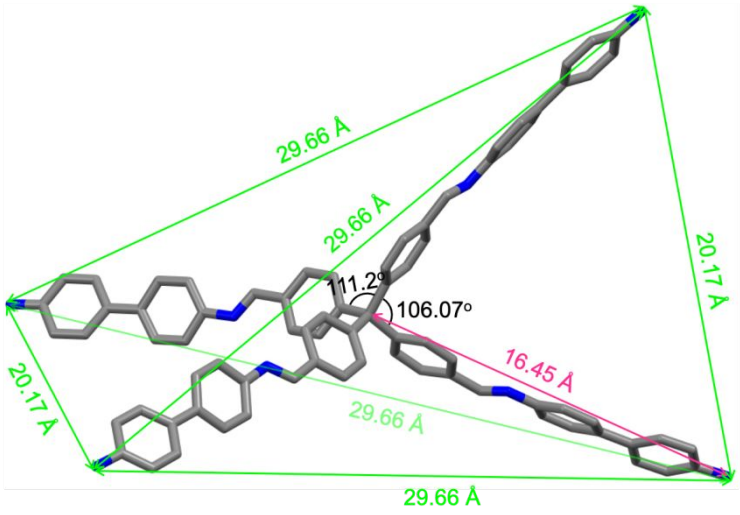

Figure S6. The single crystal molecular structure of **H2** displaying a quasi-tetrahedral conformation (C: gray, N: blue). Hydrogen atoms are omitted for clarity. The green lines show the distances between the terminal nitrogen atoms. The pink line shows the distance between the central methane carbon atom and the terminal nitrogen atoms.

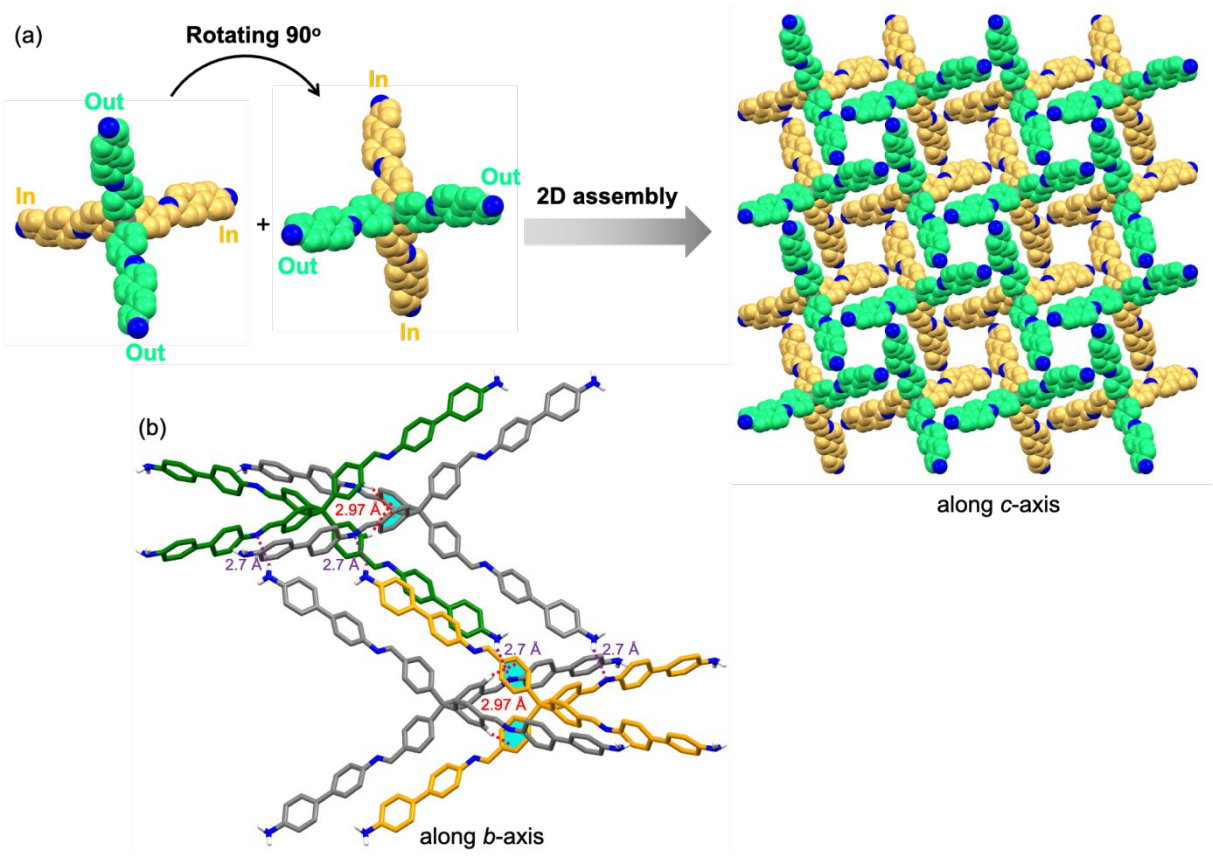

Figure S7. Crystal stacking arrangement of **H2**. (a) The 2D assembly along the *c*-axis. The directions of out (green) and in (yellow) refer to the direction of the central carbon atom. (b) View down the *b*-axis of the stacking structure. The purple and red dashed lines show the intermolecular N-H···N hydrogen bonds and C-H···π interactions, respectively. Molecular skeletons are shown in green, grey, and yellow, respectively.

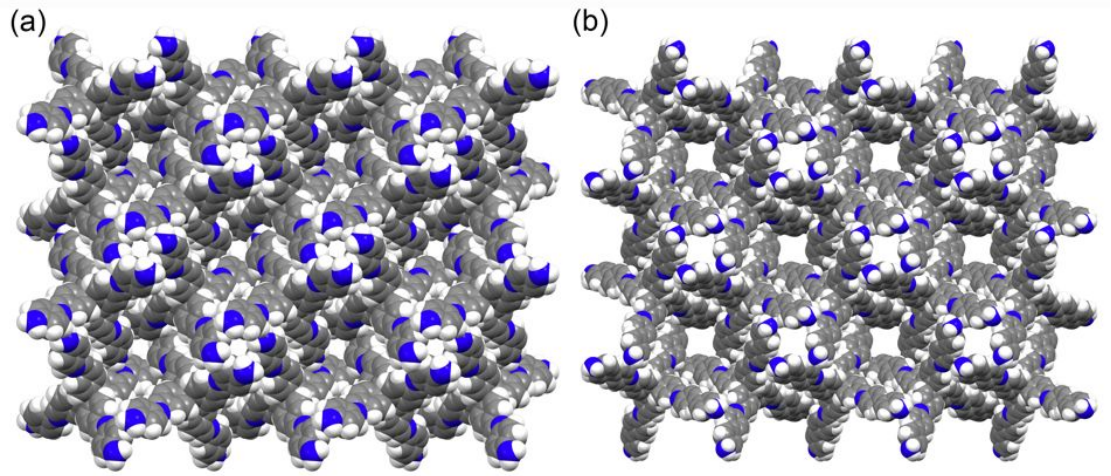

Figure S8. Space-filling model of **H1** (a) and **H2** (b) along the c-axis showing the size of the channels. The gray, blue and white spheres represent C, N and H atoms, respectively.

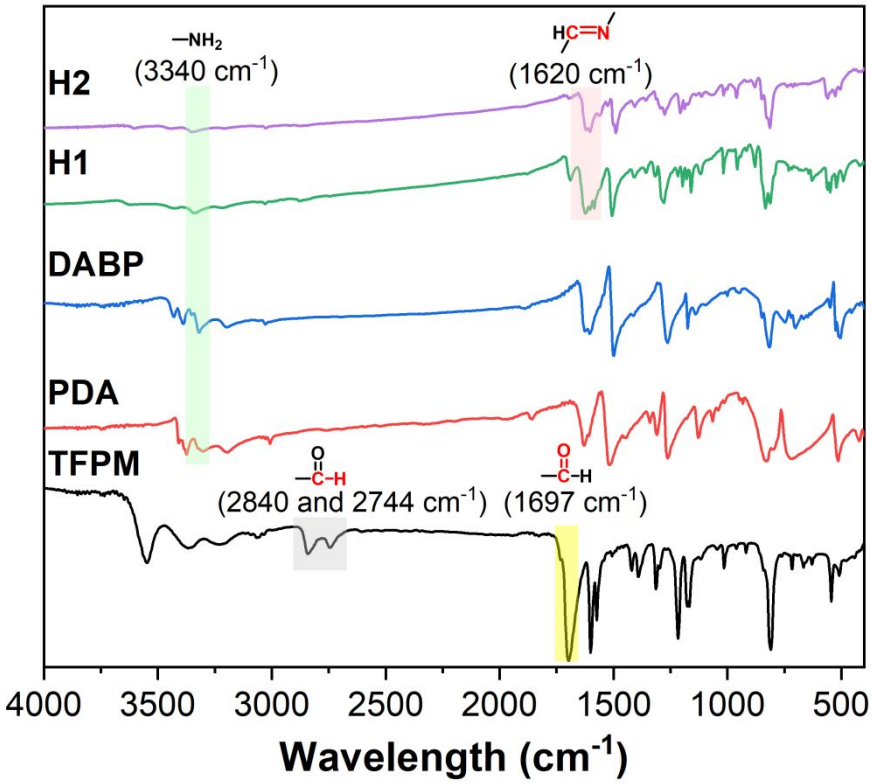

Figure S9. FT-IR spectra of **H1** and **H2** and their corresponding monomers.

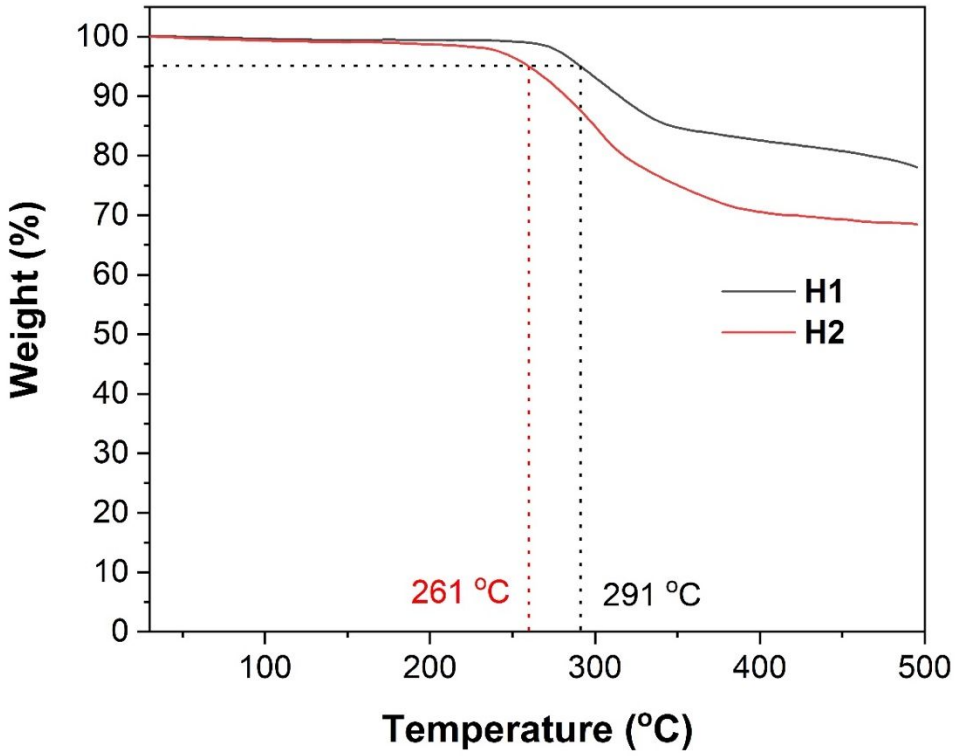

Figure S10. TGA curves for **H1** and **H2** recorded under an N_2 atmosphere with a heating rate of 10 ˚C min^{-1}.

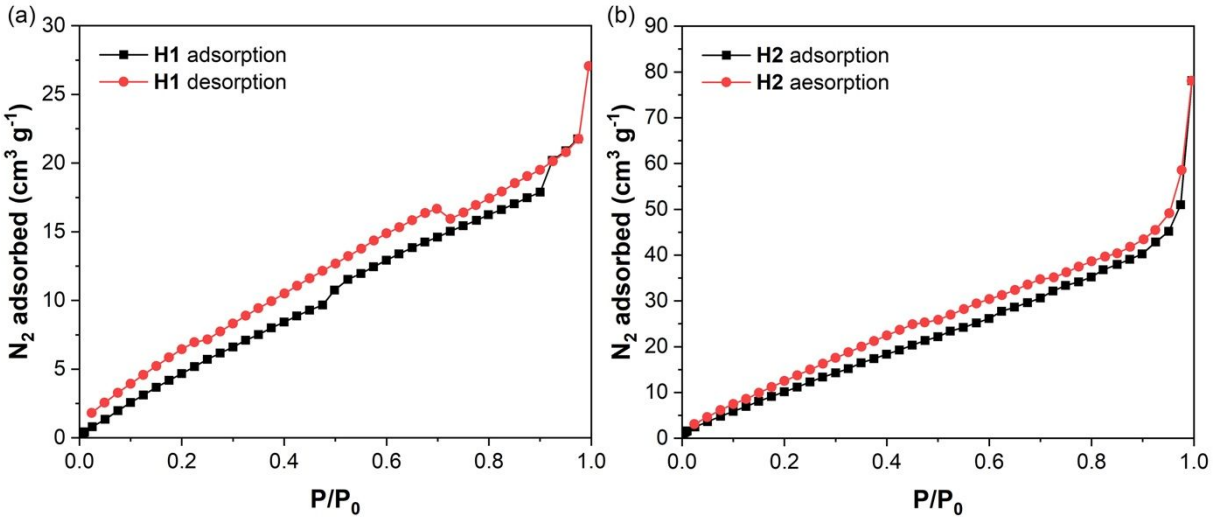

Figure S11. N_2 sorption isotherms for **H1** (a) and **H2** (b) at 77 K. Samples were activated by degassed at 100 ˚C under vacuum for 24 h prior to each N_2 adsorption and desorption analysis.

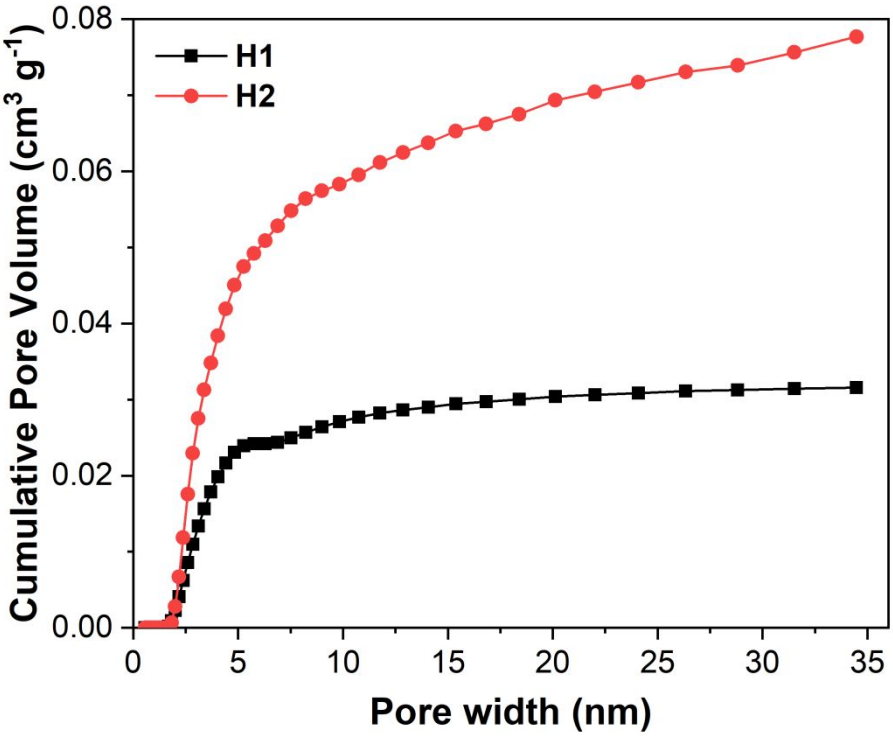

Figure S12. Cumulative pore volume analysis of **H1** and **H2** obtained using non-local density functional theory (NLDFT).

Table S5 Porosity parameters for the HOFs in the present study.

HOFs	S_{BET} ($m^2\ g^{-1}$)	Pore Volume [a] ($cm^3\ g^{-1}$)	Pore Width (nm)
H1	17.472	0.032	2.382
H2	36.755	0.078	2.6

a) Cumulative pore volume calculated by non-local density functional theory from the nitrogen adsorption/desorption experiments shown in Figure S8.

Iodine vapor uptake and release

Adsorption process: The iodine vapor adsorption capacities of the HOFs in the present study were determined by means of gravimetric analyses. The HOF sample (10 mg) was placed in 5 mL weighing vials, which were pre-weighed before testing and put in 100 mL sealed container with iodine kept at the bottom. The container was kept at 348.15 K at ambient pressure and iodine uptake was determined at different time intervals. The values of uptake capacity are the average values from at least two experiments.

Release process: The iodine-loaded HOFs (15 mg) was added into 15 mL of methanol and stirred at room temperature. After certain time intervals, 3 μL of the mixture was diluted to 3 mL by methanol and filtered. The concentration of iodine released from I_2@HOFs was recorded by the UV-Vis spectral intensity of the filtrate.

Adsorption from an aqueous iodine source phase

The HOF sample (3.0 mg) was added into an iodine aqueous solution (3.0 mL, 1.0 mM) and stirred at room temperature. After certain time intervals, the concentration of the residual iodine in aqueous solution was obtained by filtering off the HOF sample and recording the UV-Vis spectral intensity of the filtrate. Quantification was performed by comparison to a calibration curve. Removal efficiency was calculated using following equation 1:

$$\left(\text{Removal efficiency} = \frac{C_0 - C_t}{C_0} \times 100\%\right) \quad (1)$$

where C_0 (mM) and C_t (mM) are the concentrations of the iodine aqueous solution before and after treating with the HOF sample.

The amount of iodine adsorbed from the aqueous source phase was determined using the following equation 2:

$$\left(q_t = \frac{(C_0 - C_t)\ M_w}{m \times 1000}\right) \quad (2)$$

where q_t (g g^{-1}) is the amount of adsorbed iodine per g of adsorbent at time t (min). C_0 (mM) and C_t (mM) are the initial and residual concentrations of the iodine aqueous source and post HOFs treatment filtrate, respectively. M_w (g mol^{-1}) is the molecular mass of iodine; m (g g^{-1}) is the mass of the HOF used in the study.

Adsorption kinetics

Pseudo-first-order (equation 3) and pseudo-second-order (equation 4) models were used to fit the adsorption kinetics.

$$(\mathbf{ln}(\boldsymbol{q}_e - \boldsymbol{q}_t) = \mathbf{ln}\,\boldsymbol{q}_e - \boldsymbol{k}_1\boldsymbol{t}) \quad (3)$$

Where q_e and q_t represent the amount of iodine adsorption (mg g^{-1}) at equilibrium and the amount of iodine adsorbed (mg g^{-1}) at any given time, t, respectively. k_1 (min^{-1}) is the pseudo-first-order rate constant corresponding to the adsorption kinetics per this model.

$$(\frac{t}{q_t} = \frac{t}{q_e} + \frac{1}{k_{obs}\ q_e^2}) \quad (4)$$

where q_t is amount of iodine adsorbed from aqueous solution (g g^{-1}) at time t (min); q_e is the adsorbate uptake (g g^{-1}) at equilibrium. k_{obs} is a second-order rate constant (g g^{-1} min^{-1}), which can be calculated from the intercept and slope of a plot of t/q_t against t.

Iodine Adsorption Capacity from Aqueous KI/I_2 Solutions

HOF samples (50 mg) were placed in the round bottom flask containing 3.0 g KI, 1.5 g I_2 and 3 mL water. The mixture was stirred at room temperature for 48 h. The samples were collected by filtration, washed with water, and dried in the air to afford a black solid. The filtrate was collected and subjected to a bisulfite starch titration.

5 mL of a 1% aqueous starch indicator solution was added into the combined filtrate and washings, and the resulting solution slowly titrated with the 0.05 M sodium bisulfite aqueous solution until the original blue colour was disappeared. The iodine adsorption capacity of the HOFs in question was then calculated from the net change in the iodine content in the starting and post-HOF exposure aqueous solutions.

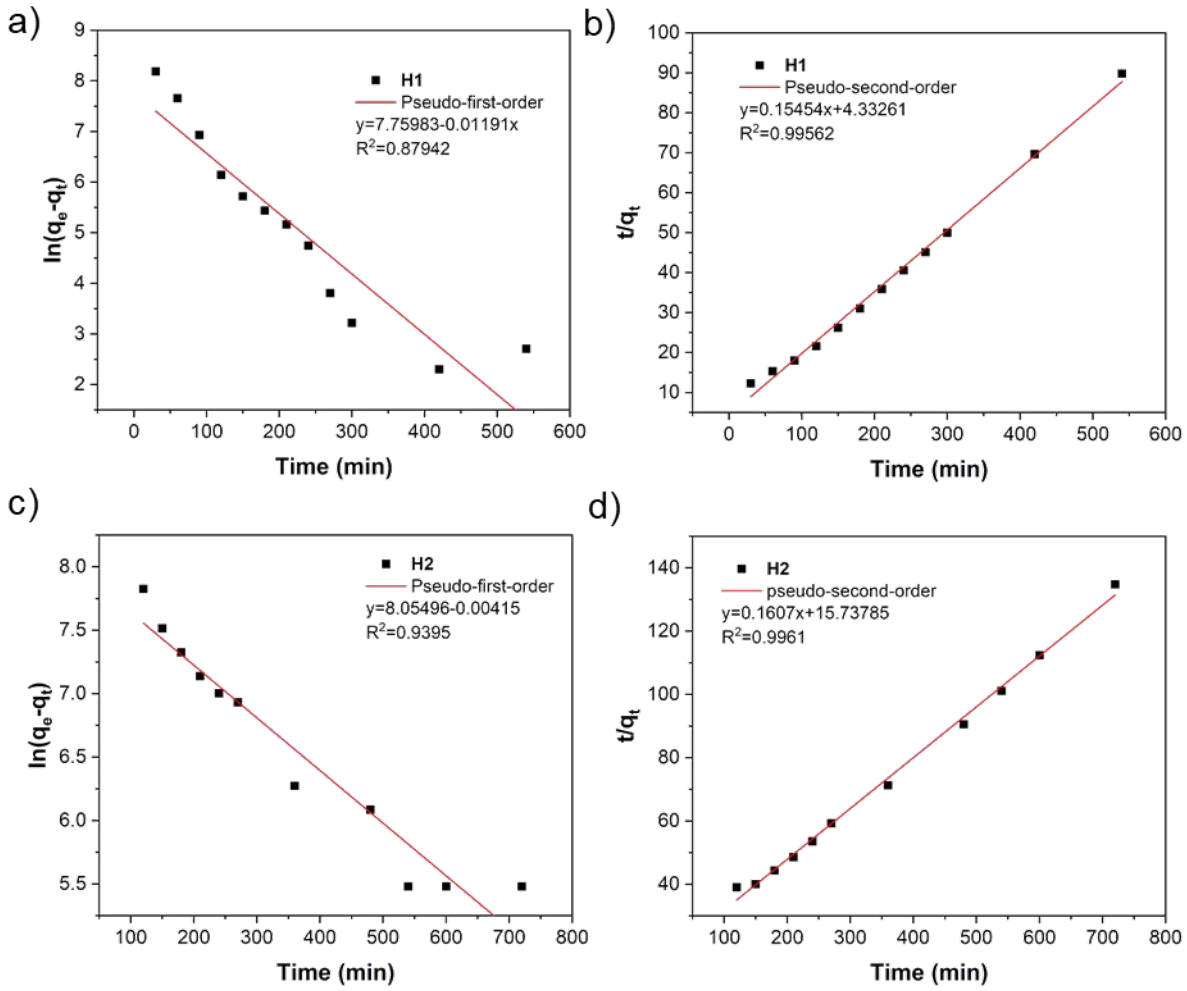

Figure S13. Pseudo-first-order and pseudo-second-order adsorption kinetic plots of iodine vapor uptake by **H1** (a and b) and **H2** (c and d), respectively.

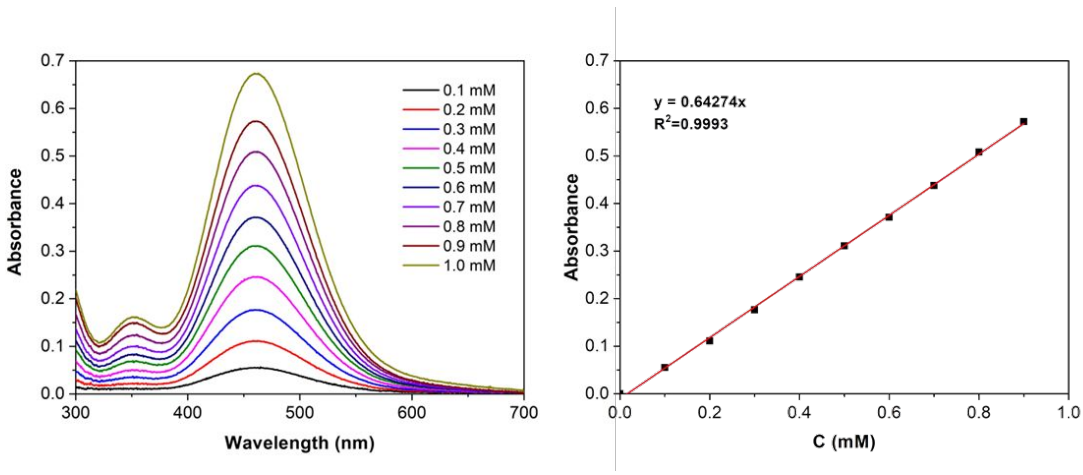

Figure S14. UV-Vis spectra of iodine aqueous solutions with different concentrations (left). Standard curve plotted based on the absorbance at 460 nm (right).

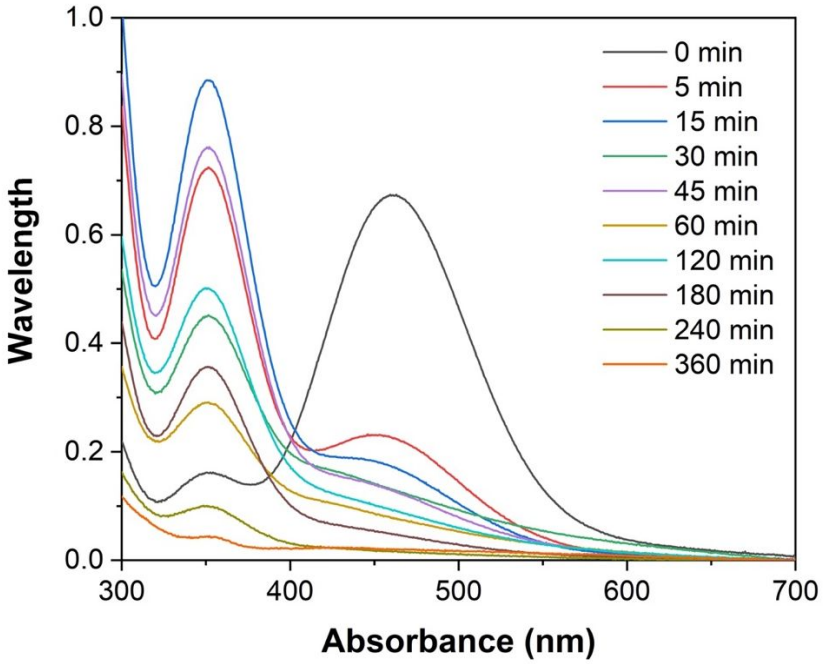

Figure S15. Time-dependent UV-Vis spectra of iodine aqueous solution (1.0 mM) upon addition of **H1** (1.0 mg mL^{-1}).

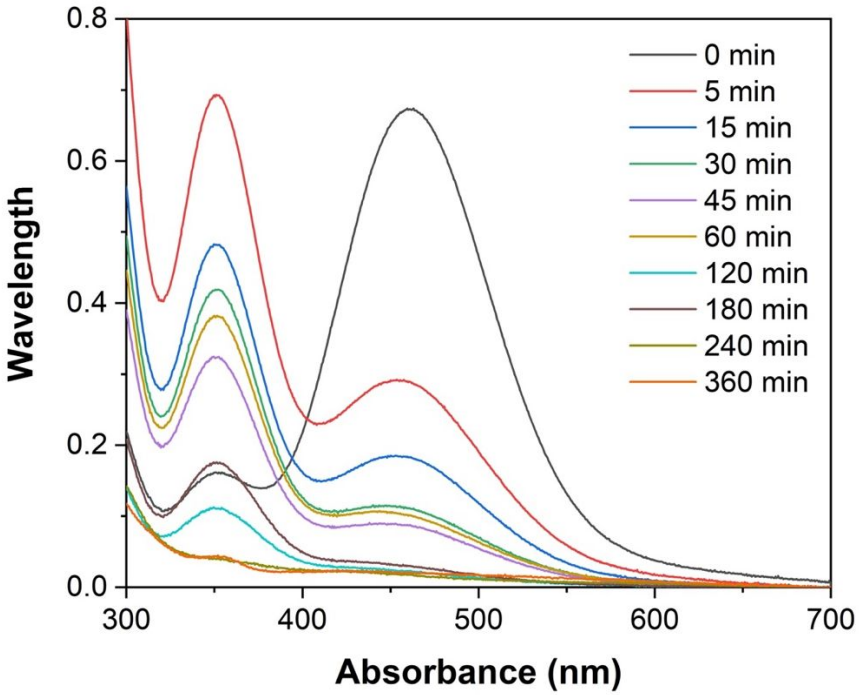

Figure S16. Time-dependent UV-Vis spectra of iodine aqueous solution (1.0 mM) upon addition of **H2** (1.0 mg mL^{-1}).

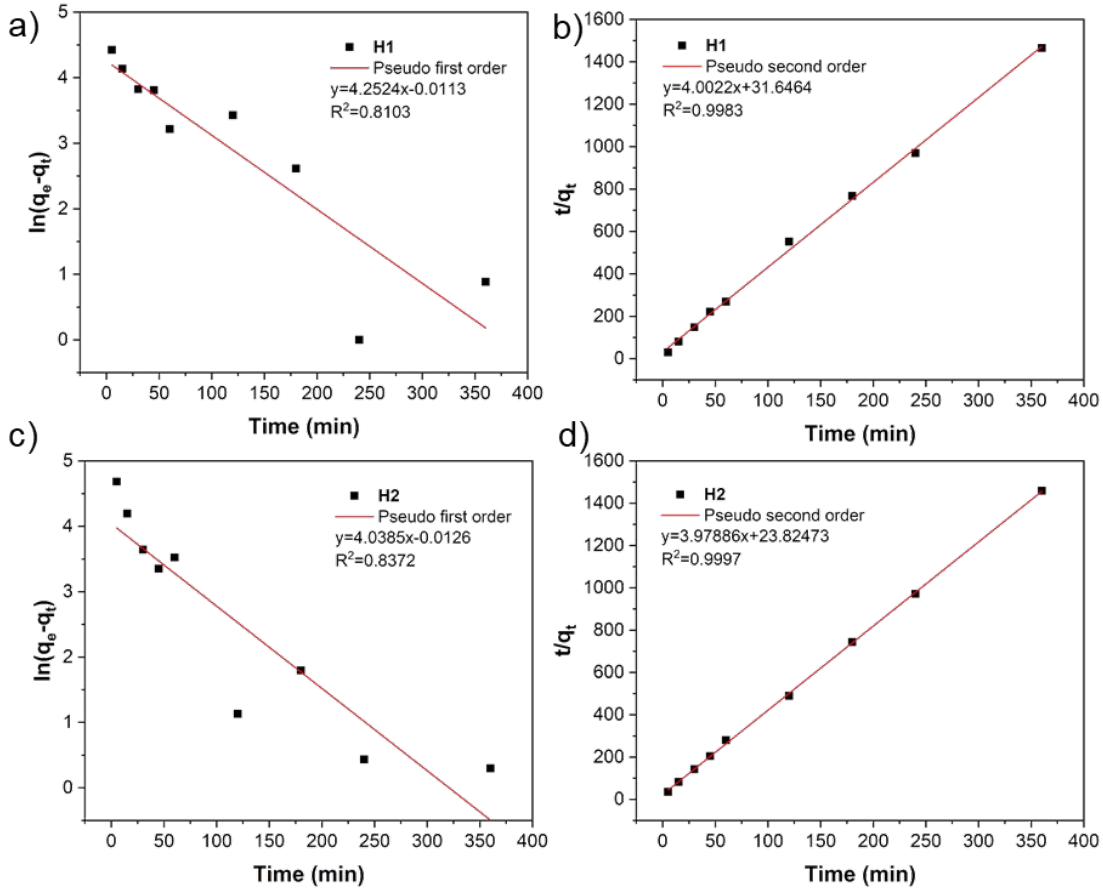

Figure S17. Pseudo-first-order and pseudo-second-order adsorption kinetic plots corresponding to the uptake of iodine from aqueous solutions (1.0 mM in all cases) by **H1** (a and b) and **H2** (c and d), respectively.

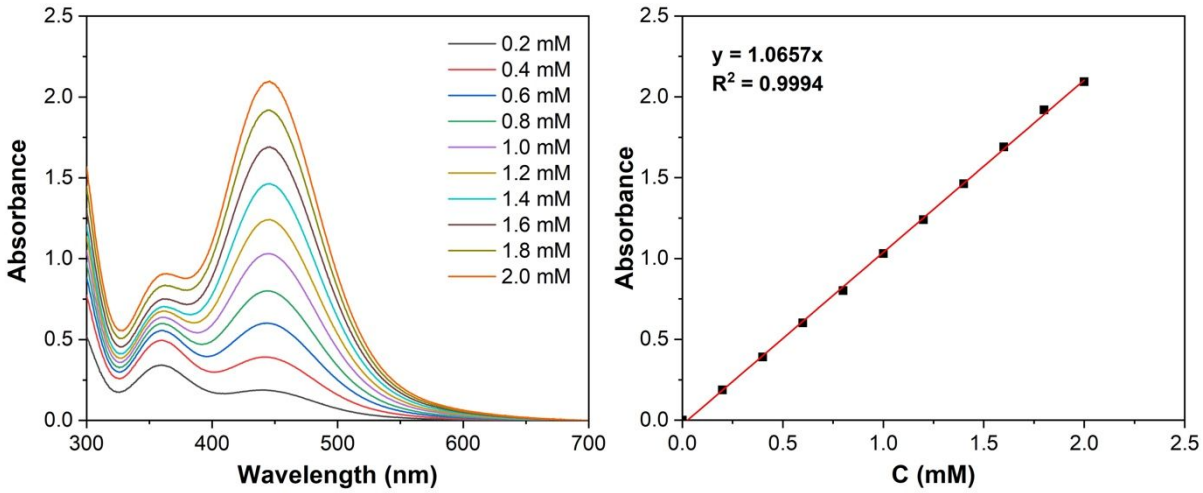

Figure S18. UV-Vis spectra of iodine methanol solutions with different concentrations (left). Standard curve plotted based on the absorbance at 444 nm (right).

Table S6. Summary of iodine adsorption capacities for the HOFs.

NO.	Material	I_2 uptake capacity in aqueous solution ($g\ g^{-1}$)	I_2 uptake capacity in vapor ($g\ g^{-1}$)	Ref.
1	**H1**	4.44	6.02	**This work**
2	**HcOF-4**	3.57	/	*J Am Chem Soc*, 2019, 141: 10915-10923.
3	**HcOF-2**	3.23	/	*J Am Che. Soc*, 2019, 141: 10915-10923.
4	**HOF_T-Hex**	3.2	6.4	*Adv Funct Mater,* 2024, 34: 2311964-2311974.
5	**HcOF-3**	3.00	/	*J Am Chem Soc*, 2019, 141: 10915-10923.
6	**H2**	2.34	5.45	**This work**
7	**HcOF-1**	2.1	/	*J Am Chem Soc*, 2017, 139: 7172-7175.
8	**HOF-TAM-BPY**	1.12	7.83	*J Mater Chem A*, 2022, 10: 18730-18736.
9	**HOF-TAM-PNA**	0.891	6.78	*J Mater Chem A*, 2022, 10: 18730-18736.
10	**HOF-TAM-BDA**	0.671	6.41	*J Mater Chem A*, 2022, 10: 18730-18736.
11	**ENTDAT**	/	1.8	*J Mater Chem C*, 2021, 9: 9932-9940.
12	**ETTA_Cl_a**	/	1.64	*Nano Res*, 2024, 17: 6766-6772
13	**HOF_T-Pr**	/	1.5	*Adv Funct Mater,* 2024, 34: 2311964-2311974.
14	**HOF_B-Hex**	/	0.92	*Adv Funct Mater,* 2024, 34: 2311964-2311974.
15	**ETTA_Br_a**	/	0.56	*Nano Res*, 2024, 17: 6766-6772

NMR spectra of the β-iodoether products

(2-Iodo-1-methoxyethane-1,1-diyl)dibenzene (1a): ^{1}H NMR (400 MHz, $CDCl_3$) δ 7.40-7.24 (m, 10H), 4.15-4.10 (s, 2H), 3.15-3.10 (s, 3H). ^{13}C NMR (101 MHz, $CDCl_3$) δ 16.01, 50.50, 80.77, 127.15, 127.43, 128.20, 142.98.

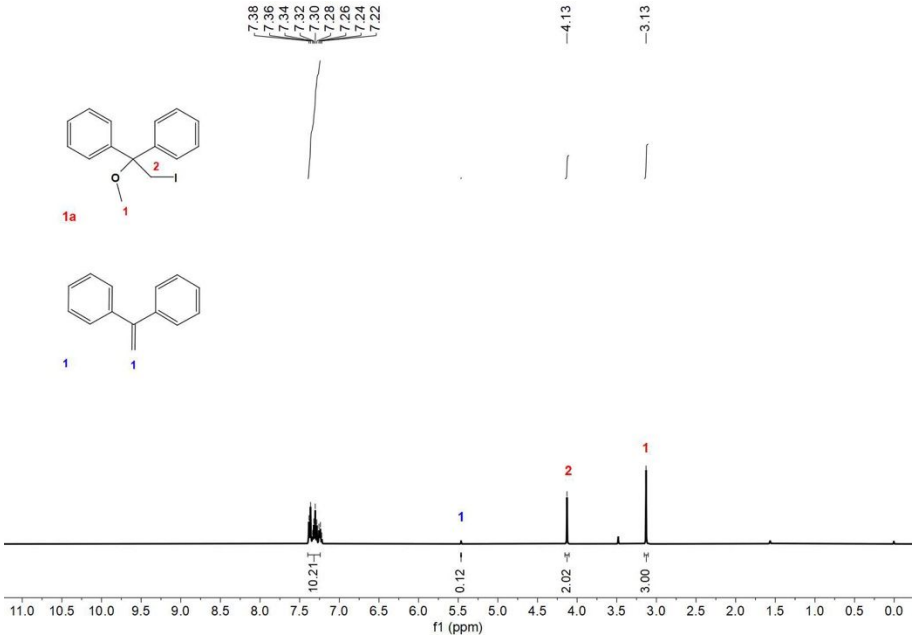

Figure S19. ^{1}H NMR spectrum of **1a** with internal standard of methyl benzoate in $CDCl_3$. The red and blue numbers show the assignment of Markovnikov product **1a** and reactant **1**, respectively.

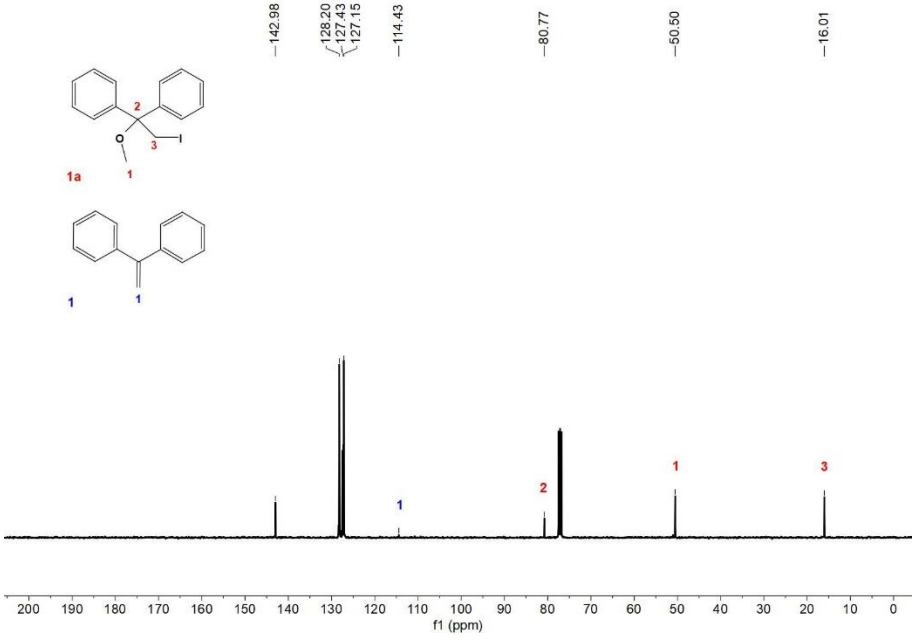

Figure S20. ^{13}C NMR spectrum of **1a** with internal standard of methyl benzoate in $CDCl_3$. The red and blue numbers show the assignment of Markovnikov product **1a** and reactant **1**, respectively.

1-Iodo-2-methoxyoctane (**2a**): ^{1}H NMR (400 MHz, $CDCl_3$) δ 3.38-3.37 (s, 1H), 3.37-3.35 (s, 3H), 3.31-3.21 (m, 2H), 3.04-2.97 (m, 1H), 1.59-1.54 (d, J= 13.7 Hz, 2H), 1.35-1.22 (m, 10H), 0.90-0.85 (m, 4H). ^{13}C NMR (101 MHz, $CDCl_3$) δ 10.05, 14.16, 22.67, 25.21, 29.30, 31.83, 34.41, 57.10, 79.85.

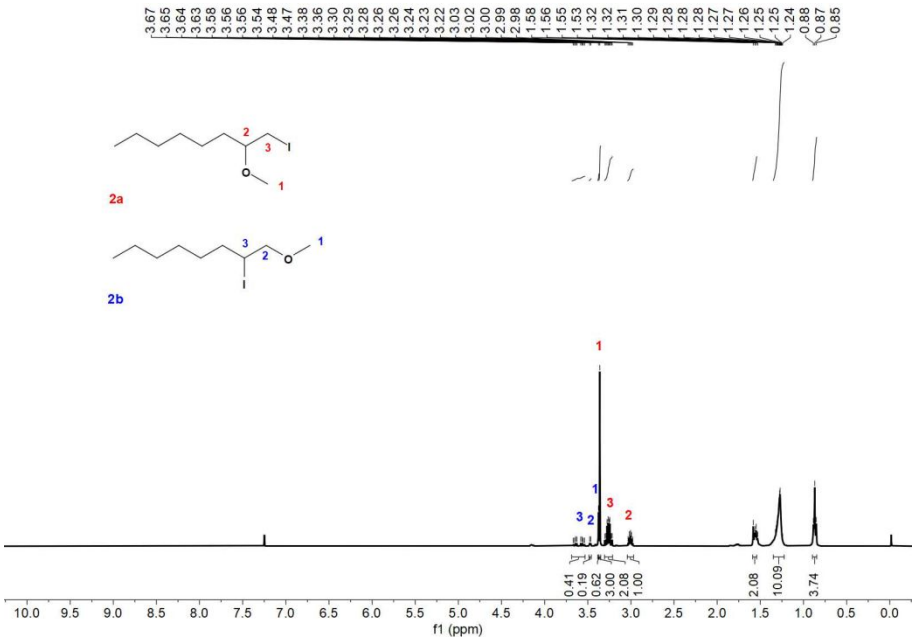

Figure S21. ^{1}H NMR spectrum of **2a** with internal standard of methyl benzoate in $CDCl_3$. The red and blue numbers show the assignment of Markovnikov product **2a** and anti-Markovnikov product **2b**, respectively.

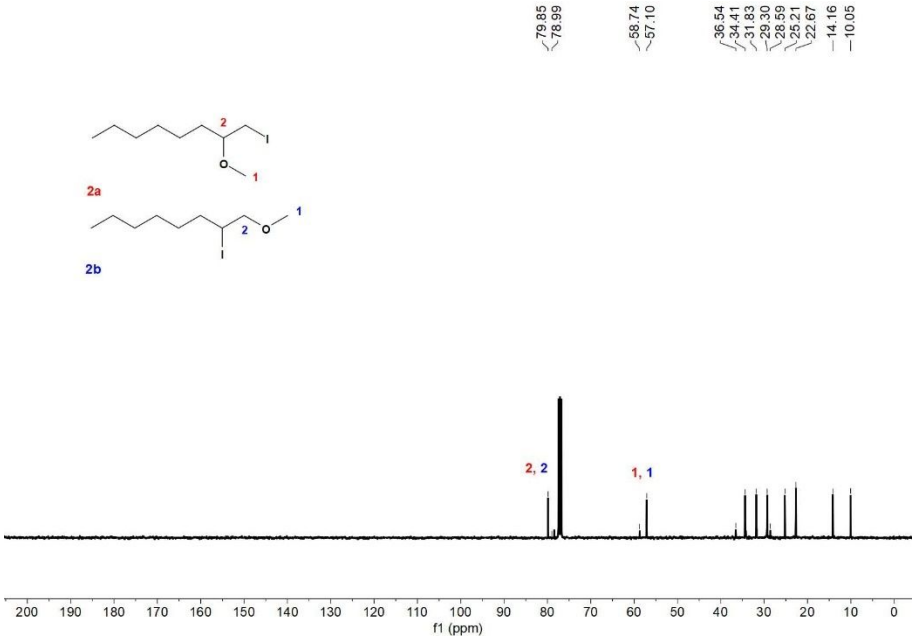

Figure S22. ^{13}C NMR spectrum of **2a** with internal standard of methyl benzoate in $CDCl_3$. The red and blue numbers show the assignment of Markovnikov product **2a** and anti-Markovnikov product **2b**, respectively.

1-Iodo-2-methoxydodecane (3a): ^{1}H NMR (400 MHz, $CDCl_3$) δ 3.37 (s, 3H), 3.32-3.22 (m, 2H), 3.05-2.98 (m, 1H), 1.61-1.53 (q, J = 7.6, 7.0 Hz, 2H), 1.34-1.21 (d, J = 6.4 Hz, 16H), 0.90-0.84 (t, J = 6.7 Hz, 3H). ^{13}C NMR (101 MHz, $CDCl_3$) δ 10.01, 14.21, 22.78, 25.25, 29.42, 29.66, 31.99, 34.40, 57.09, 79.86.

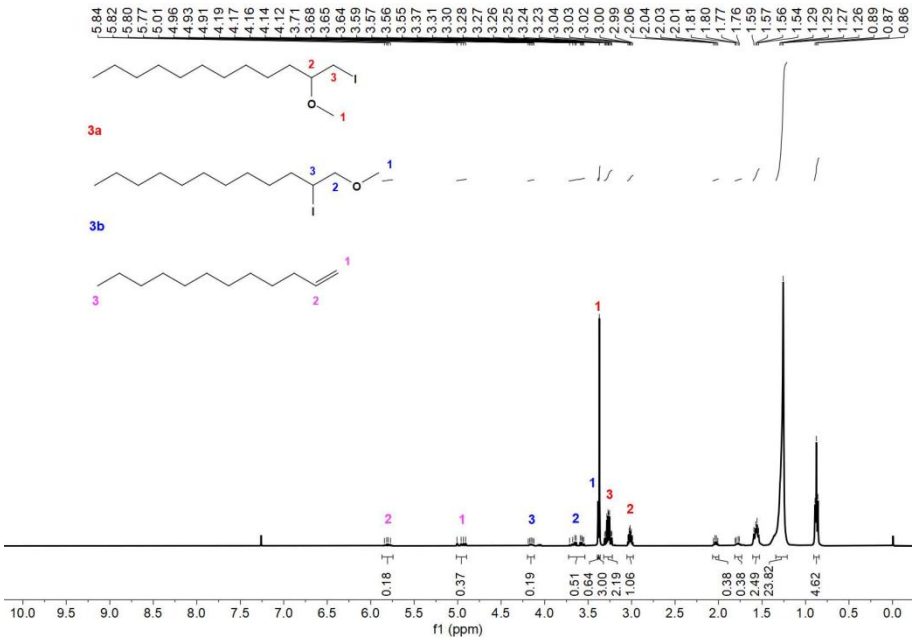

Figure S23. ^{1}H NMR spectrum of **3a** with internal standard of methyl benzoate in $CDCl_3$. The red, blue and pink numbers show the assignment of Markovnikov product **3a**, anti-Markovnikov product **3b** and reactant **3**, respectively.

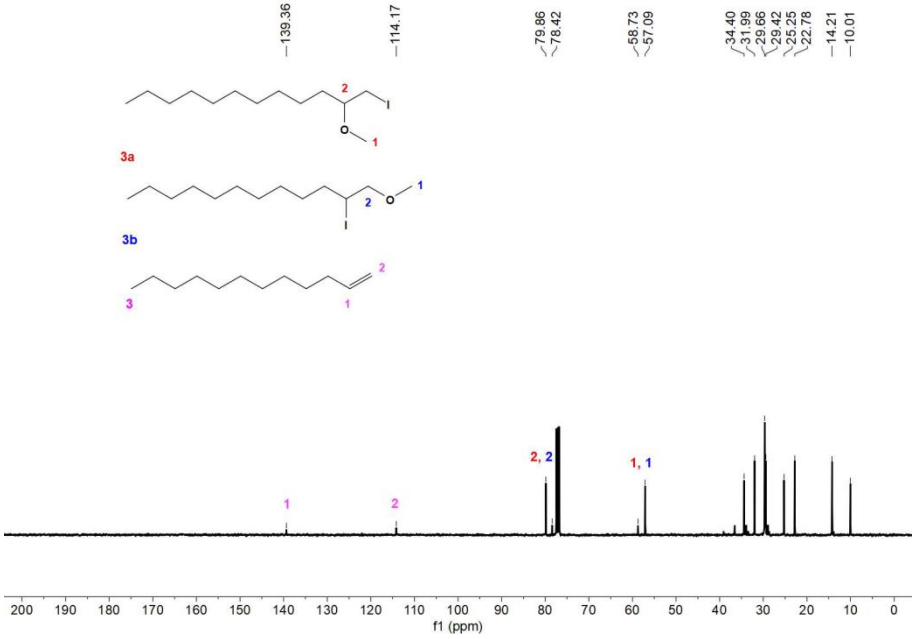

Figure S24. ^{13}C NMR spectrum of **3a** with internal standard of methyl benzoate in $CDCl_3$. The red, blue and pink numbers show the assignment of Markovnikov product **3a**, anti-Markovnikov product **3b** and reactant **3**, respectively.

(2-Iodo-1-methoxyethyl)benzene (4a): ^{1}H NMR (400 MHz, $CDCl_3$) δ 7.39-7.28 (m, 5H), 4.31-4.26 (dd, J = 7.8, 5.0 Hz, 1H), 3.36-3.31 (m, 2H), 3.30-3.29 (s, 3H). ^{13}C NMR (101 MHz, $CDCl_3$) δ 10.57, 57.42, 83.67, 126.66, 128.55, 128.81, 139.86.

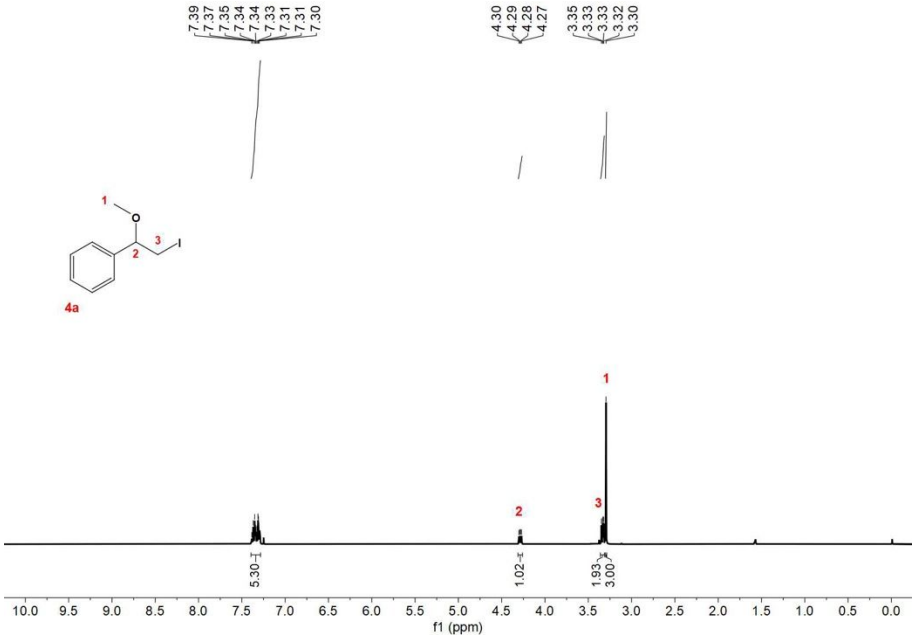

Figure S25. ^{1}H NMR spectrum of **4a** with internal standard of methyl benzoate in $CDCl_3$. The red numbers show the assignment of Markovnikov product **4a**.

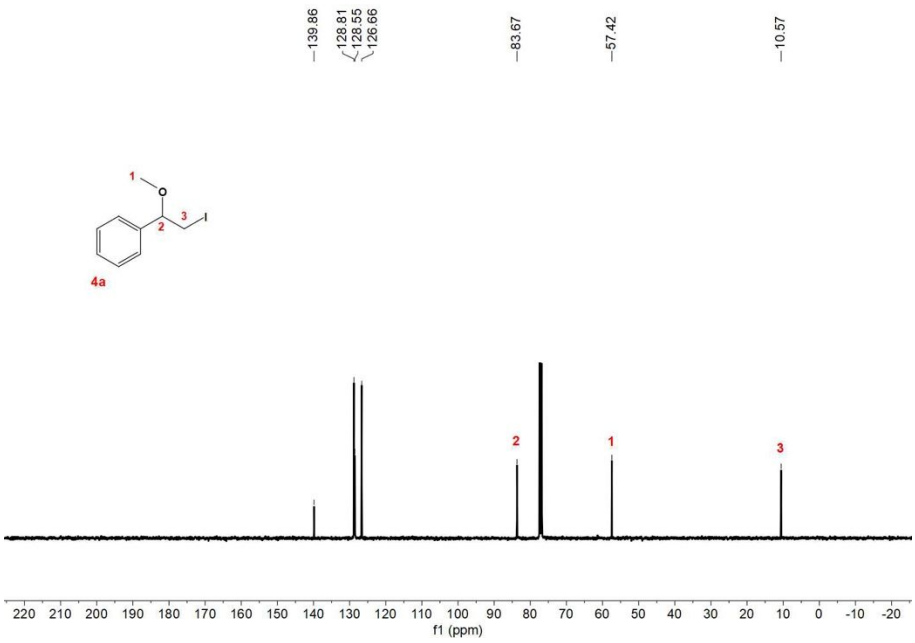

Figure S26. ^{13}C NMR spectrum of **4a** with internal standard of methyl benzoate in $CDCl_3$. The red numbers show the assignment of Markovnikov product **4a**.

(1-Iodo-2-methoxypropan-2-yl)benzene (5a): ^{1}H NMR (400 MHz, $CDCl_3$) δ7.42-7.26 (m, 5H), 3.53-3.41 (m, 2H), 3.15-3.11 (s, 3H), 1.72-1.68 (s, 3H). ^{13}C NMR (101 MHz, $CDCl_3$) δ19.84, 23.96, 51.39, 77.08, 126.41, 127.87, 128.60, 141.51.

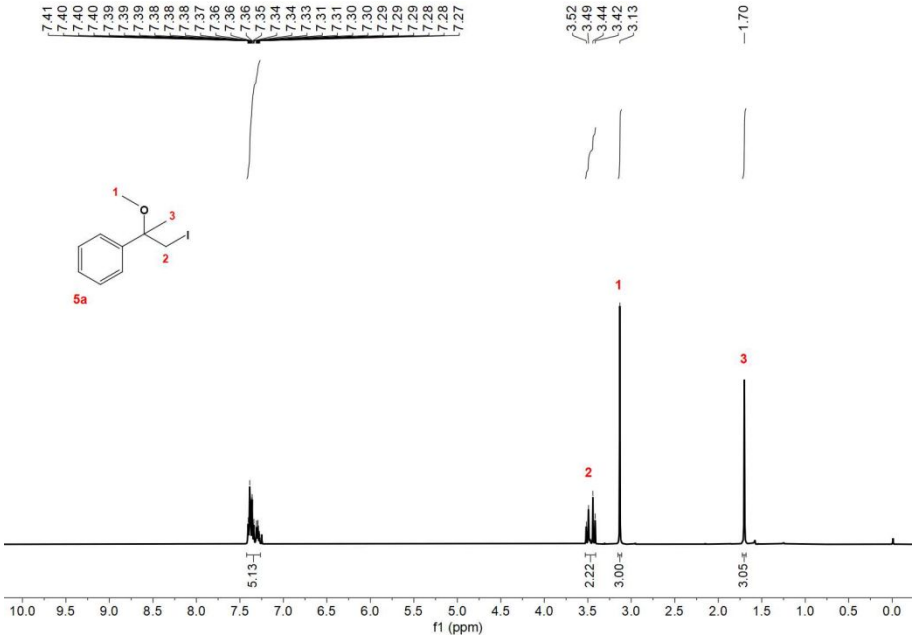

Figure S27. ^{1}H NMR spectrum of **5a** with internal standard of methyl benzoate in $CDCl_3$. The red numbers show the assignment of Markovnikov product **5a**.

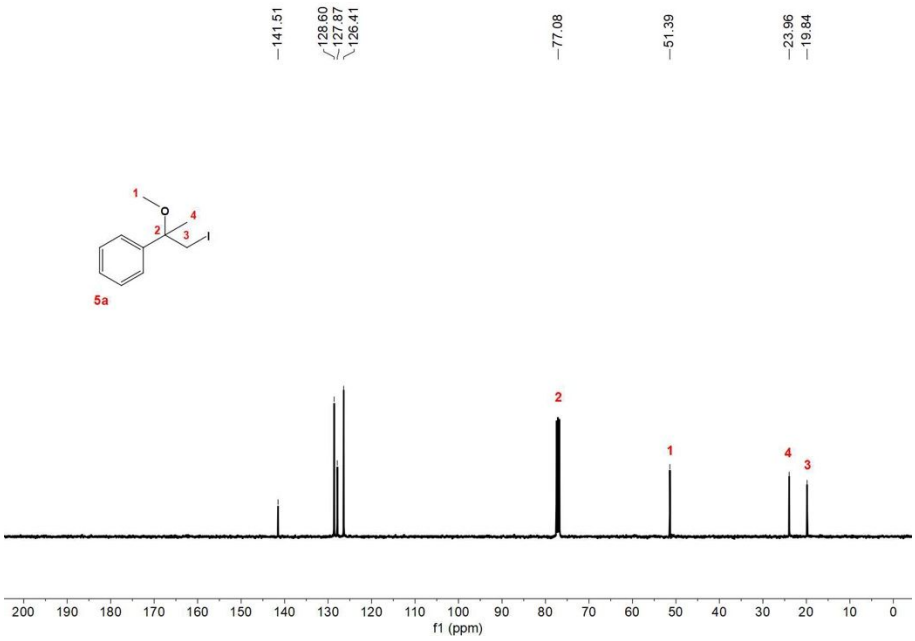

Figure S28. ^{13}C NMR spectrum of **5a** with internal standard of methyl benzoate in $CDCl_3$. The red numbers show the assignment of Markovnikov product **5a**.

1-Iodo-2-methoxycyclohexane (6a): ^{1}H NMR (400 MHz, $CDCl_3$) δ 4.09-3.99 (ddd, J = 10.7, 8.7, 4.3 Hz, 1H), 3.42-3.35 (s, 3H), 3.26-3.17 (td, J = 8.9, 4.0 Hz, 1H), 2.42-2.33 (m, 1H), 2.21-2.12 (m, 1H), 2.01-1.87 (dtd, J = 14.4, 10.8, 3.8 Hz, 1H), 1.85-1.75 (m, 1H), 1.56-1.46 (m, 1H), 1.39-1.19 (m, 3H). ^{13}C NMR (101 MHz, $CDCl_3$) δ 23.64, 27.24, 30.39, 35.51, 37.90, 56.92, 84.03.

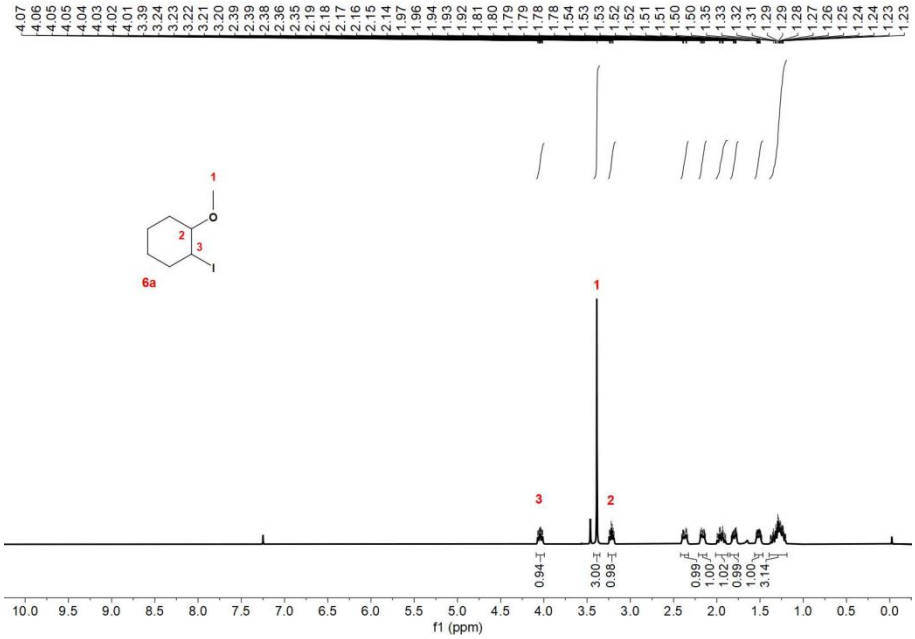

Figure S29. ^{1}H NMR spectrum of **6a** with internal standard of methyl benzoate in $CDCl_3$. The red numbers show the assignment of Markovnikov product **6a**.

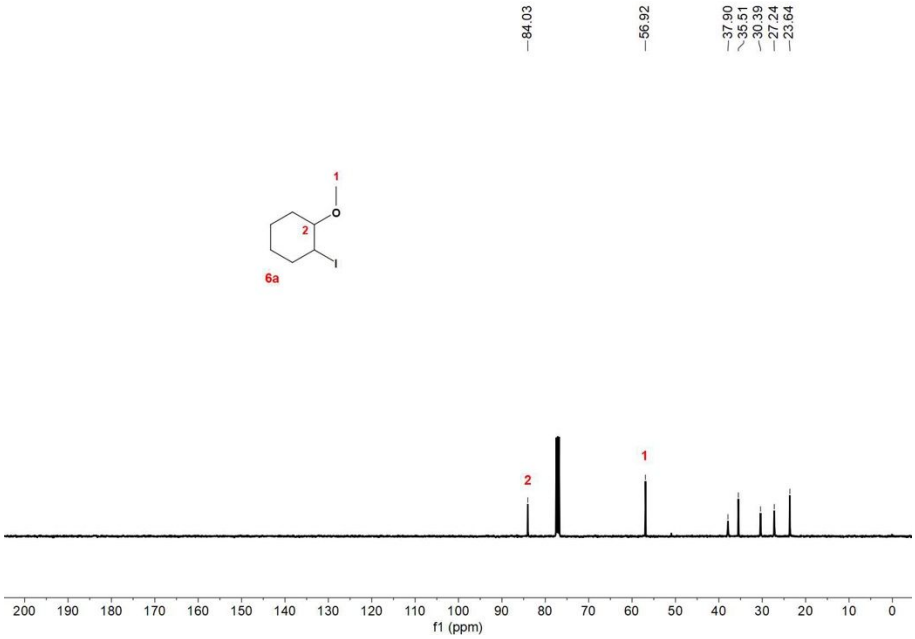

Figure S30. ^{13}C NMR spectrum of **6a** with internal standard of methyl benzoate in $CDCl_3$. The red numbers show the assignment of Markovnikov product **6a**.

2-Iodo-1-methoxy-1-methylcyclohexane (7a): ^{1}H NMR (400 MHz, $CDCl_3$) δ 4.39-4.33 (dd, J = 9.8, 4.1 Hz, 1H), 3.24-3.19 (s, 3H), 2.34-2.24 (m, 1H), 2.05-1.93 (ddt, J = 15.0, 10.2, 4.9 Hz, 2H), 1.76-1.67 (m, 1H), 1.63-1.56 (m, 2H), 1.46-1.34 (m, 2H), 1.33-1.31 (s, 3H). ^{13}C NMR (101 MHz, $CDCl_3$) δ 22.50, 22.88, 26.65, 32.98, 36.22, 42.56, 48.83, 75.87.

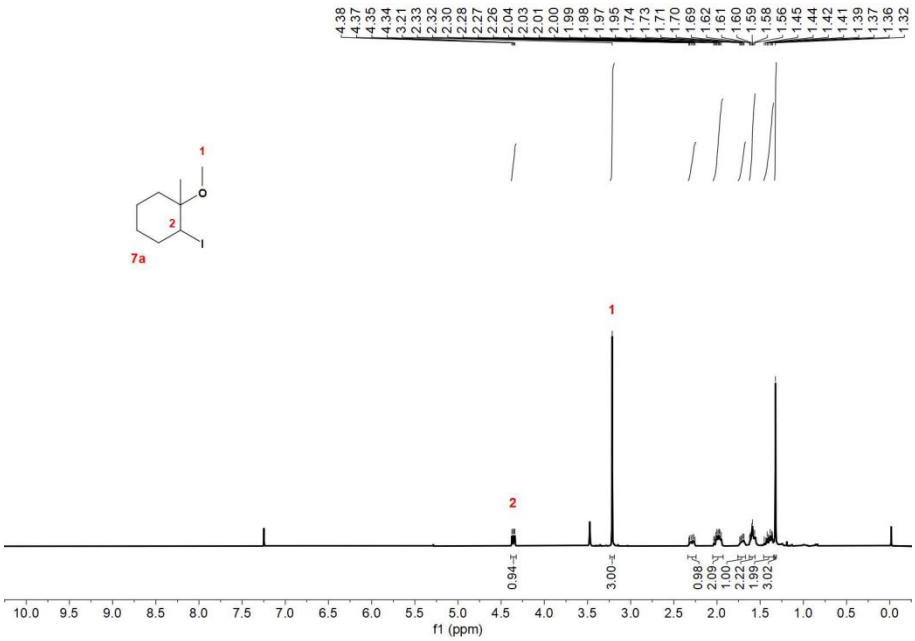

Figure S31. ^{1}H NMR spectrum of **7a** with internal standard of methyl benzoate in $CDCl_3$. The red numbers show the assignment of Markovnikov product **7a**.

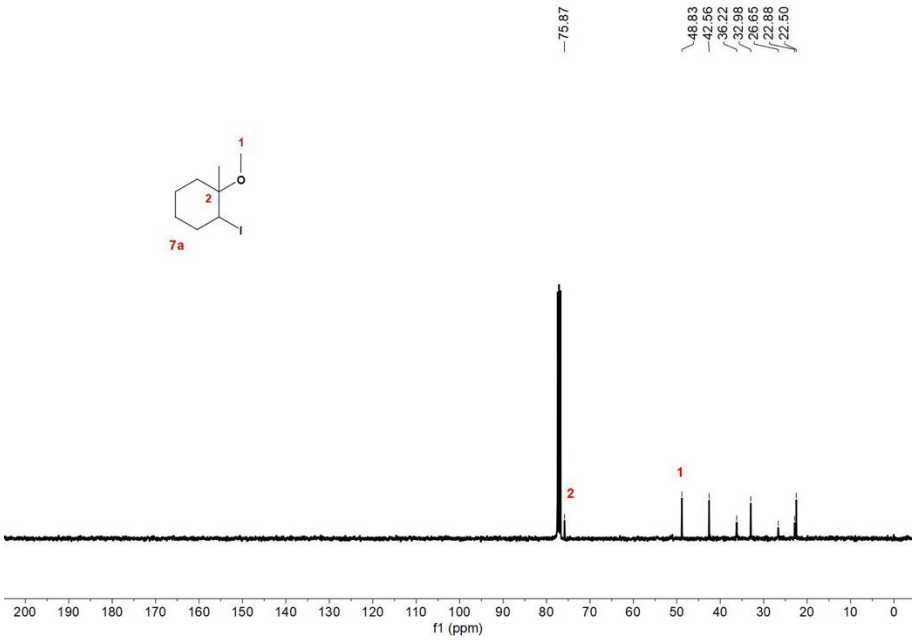

Figure S32. ^{13}C NMR spectrum of **7a** with internal standard of methyl benzoate in $CDCl_3$. The red numbers show the assignment of Markovnikov product **7a**.

1-Iodo-2-methoxy-3-methylcyclohexane (8a): ^{1}H NMR (400 MHz, $CDCl_3$) δ 4.58-4.54 (s, 1H), 3.75-3.71 (q, J = 3.5 Hz, 1H), 3.38-3.34 (s, 3H), 2.24-2.14 (m, 1H), 1.77-1.68 (m, 1H), 1.64-1.56 (m, 1H), 1.52-1.45 (dt, J = 13.3, 4.0 Hz, 1H), 1.42-1.34 (m, 1H), 1.29-1.14 (m, 2H), 0.95-0.90 (d, J = 6.1 Hz, 3H). ^{13}C NMR (101 MHz, $CDCl_3$) δ 20.27, 23.67, 24.62, 30.10, 31.63, 46.62, 56.89, 81.34.

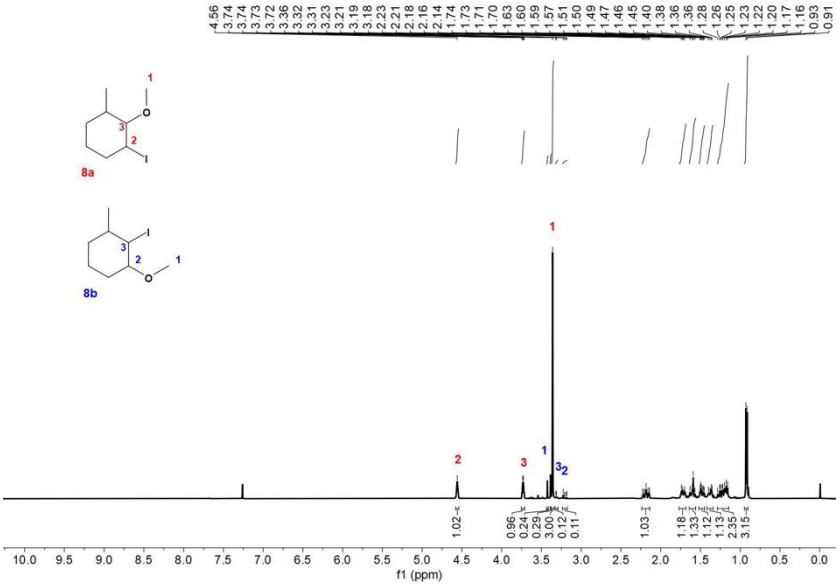

Figure S33. ^{1}H NMR spectrum of **8a** with internal standard of methyl benzoate in $CDCl_3$. The red and blue numbers show the assignment of Markovnikov product **8a** and anti-Markovnikov product **8b**, respectively.

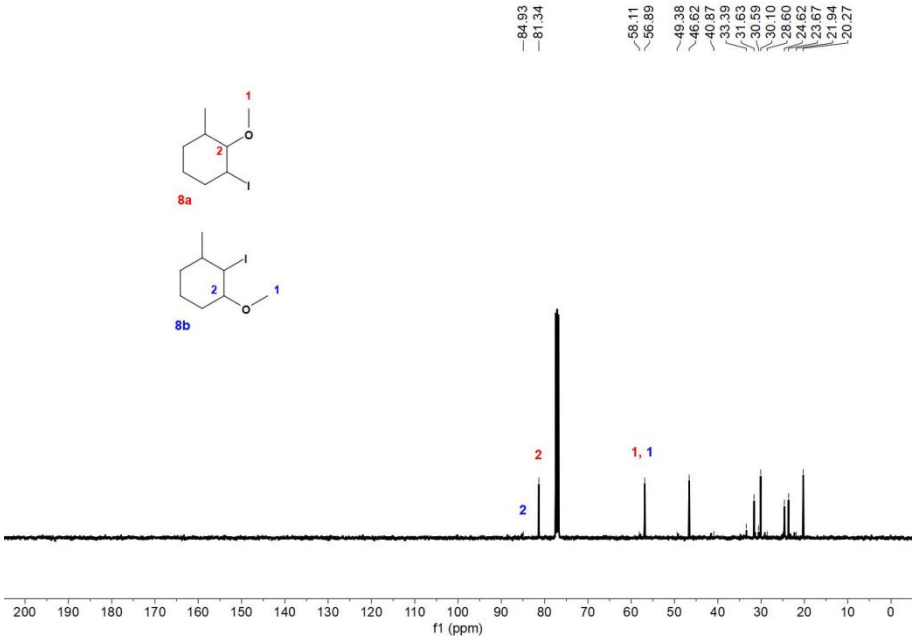

Figure S34. ^{13}C NMR spectrum of **8a** with internal standard of methyl benzoate in $CDCl_3$. The red and blue numbers show the assignment of Markovnikov product **8a** and anti-Markovnikov product **8b**, respectively.